Surface Segregation of Methyl Side Branches Monitored by Sum Frequency Generation (SFG) Vibrational Spectroscopy for a Series of Random Poly(ethylene-*co*-propylene) Copolymers

Aric Opdahl,[†] Roger A. Phillips,[‡] and Gabor A. Somorjai*[,†]

Department of Chemistry, University of California at Berkeley, and Materials Science Division, Lawrence Berkeley National Laboratory, Berkeley, California 94720, Research & Development Center, Basell USA Incorporated, 912 Appleton Road, Elkton, Maryland 21921

Received: October 8, 2001; In Final Form: January 23, 2002

The surface composition and surface chain conformation of a series of random aspecific poly(ethylene-*co*-propylene) rubber copolymers *(a*EPR*)* was quantified by sum frequency generation surface vibrational spectroscopy (SFG). All of the copolymers are found to preferentially orient side-branch methyl groups out of the surface. As the ethylene content of the copolymer increases, the number of methyl groups contributing to the sum frequency signal decreases. However, the percentage of methyl groups oriented out of the surface, relative to the bulk concentration of methyl groups, increases. This surface excess of oriented methyl groups is proposed to be a result of decreased steric hindrances between adjacent methyl groups in ethylene-rich copolymers. Additionally, analysis of the CH_2 bands in the SFG spectra suggests that the CH_2 units at the surface become more oriented toward the surface normal and adopt a trans configuration as the ethylene content increases.

Introduction

Polyolefins represent model systems for studying the effects of chain architecture on surface structure, as variables including the number of short chain branches, the length of chain branches, and polymer tacticity can be isolated. The effect of short-chain branch content on surface structure and surface configuration is particularly interesting in the context of experimental studies which suggest that species with higher branch content segregate to the air/polymer surface in polyolefin blends.[1] While enthalpic arguments have been made to explain the relative surface affinities, the details of the surface configuration as a function of branch content for the pure components has not been extensively explored and may give additional insights to the segregation behavior. In the experiments presented here, the effect of the number density of methyl side branches on the surface structure has been studied.

A series of random aspecific poly(ethylene-*co*-propylene) copolymers *(a*EPR*)*, having the basic structure shown in Figure 1, was synthesized and the surface structures were characterized by sum frequency generation vibrational spectroscopy (SFG). The ethylene mole fraction randomly incorporated in the backbone was varied from 0% to 42% (increasing the ethylene content of the copolymer decreases the number density of methyl side branches). The aspecific placement of propylene monomers removes complications arising from crystallinity.

SFG has recently been developed as a technique for studying polymer surface structure. A second-order nonlinear optical process, SFG is forbidden in materials that are isotropic or randomly oriented. However, if a material that is oriented randomly in the bulk exhibits preferential ordering at the interface, then a sum frequency signal can be generated from those interfacial molecules. The technique is therefore sensitive to the number density of molecules at an interface and to the ordering of those molecules. SFG signals from thin film amorphous polymers have been shown to arise primarily from oriented chain segments in the polymer/air interfacial region.[2]

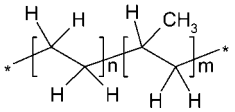

Figure 1. Structure of aspecific poly(ethylene-*co*-propylene) rubber (*a*EPR). The distribution of block lengths (*n*,*m*) is very nearly random and methyl group placement in the propylene units lack stereospecificity.

Previous SFG studies of polypropylene have shown that, in general, the methyl side branches tend to point out from the air/polymer interface.[3] The tendency of side branches to order out of the air/polymer interface is a general phenomenon observed on many polymers by SFG. Recent SFG studies on polystyrene indicate that the pendant phenyl group also orients away from the surface.[4,5] On polyimide surfaces it has been found that hydrophobic side chains orient out of the surface.[6] For polypropylene it was also shown that tacticity is important in determining the surface orientation of methyl groups.[3] Additionally, it has been shown that the methyl side branches assume different configurations above and below the glass transition temperature, T_g.[7]

SFG spectra are used in these experiments to quantify relative changes in number density and orientation of methyl side branches and methylene backbone units at the air/polymer interface for a series of *a*EPR copolymers varying in ethylene content. Methyl groups are found to preferentially order at the surface regardless of copolymer composition. The presence of ethylene units in the backbone does not change the methyl orientation at the surface significantly but does allow the CH_2 backbone to better order.

* Corresponding author. Fax: 510-643-9665. E-mail: somorjai@socrates.berkeley.edu.

[†] Department of Chemistry, University of California at Berkeley, and Materials Science Division, Lawrence Berkeley National Laboratory.

[‡] Research & Development Center, Basell USA Incorporated.

10.1021/jp013741a CCC: $22.00
Published on Web 04/30/2002

TABLE 1: Structural Characteristics of *a*PP1 and the *a*EPR Copolymers

sample	M_w	M_w/M_n	wt % ethylene	mole fraction ethylene	$[CH_2]/[CH_3]_{bulk}$	sequence parameter[b]
*a*PP1[a]	54000	2.0	0	0	1	
*a*EPR2	48000	2.0	4.7	0.069	1.15	1.0
*a*EPR3	54000	2.0	7.1	0.103	1.23	1.0
*a*EPR4	54000	2.0	13.5	0.190	1.47	1.1
*a*EPR5	48000	2.1	20.3	0.277	1.76	1.3
*a*EPR6	54000	2.0	25.9	0.344	2.05	1.3
*a*EPR7	54000	1.9	32.3	0.417	2.43	1.4

[a] 16% iso triads, 49% hetero triads, 35% syndio triads. [b] The sequence parameter, determined by NMR, is a measure of the randomness of the copolymer. It is 1 for a completely *random* distribution of co-monomers, 2 for complete *alternation* of co-monomers, and 0 for complete *block*-like sequencing.

From the calculated orientation parameters for the methyl and methylene groups, we are able to deduce relative changes in the number density of methyl groups at the surface and changes in the conformation of surface chain segments. In general, inserting ethylene units into the polymer backbone decreases the steric hindrances between adjacent methyl groups. This is proposed to allow the ethylene-rich copolymers to have more chain segments in trans configurations at the surface and to assume configurations that orient a relative surface excess of methyl groups out of the surface.

Experimental Section

Polymers. Table 1 summarizes the samples used in this study. The results in Table 1 suggest that the distribution of block lengths (*n*,*m*) in Figure 1 is very nearly random and methyl group placement in the propylene units lacks stereospecificity. Dibutylsilylbis(9-fluorenyl)zirconium dichloride catalyst was used to prepare the atactic polypropylene homopolymer (*a*PP1) and aspecific ethylene/propylene copolymers/rubber (*a*EPR2-7) in hexane with a methylaluminoxane (MAO) activator at 70 °C polymerization temperature and a molar [Al]/[Zr] ratio of 2000−3000. Closely related analogues to this aspecific catalyst have been published previously.[8] The *a*EPR copolymers were prepared by maintaining a constant monomer feed ratio. Differential Scanning Calorimetry analysis of the copolymers showed a single, composition-dependent glass transition temperature with no evidence of crystallinity for each copolymer. The as-polymerized polymers were dissolved in hexane solutions, filtered to remove large-scale polymerization impurities, and recovered by evaporation of solvent.

The tacticity and composition of *a*PP and each *a*EPR copolymer was determined by ^{13}CNMR using a Varian UNITY-300 spectrometer at 75.4 MHz in 10% *o*-dichlorobenzene solutions at 130 °C. Ethylene content was determined from the compositional triads. The NMR sequence parameter (*s.p.*), determined from compositional diads, is given in Table 1 and has a value of 1 for a random distribution of comonomers, >1 for alternating sequencing (*s.p.* = 2 for complete alternation), and <1 for blocklike sequencing (*s.p.* = 0 for complete blocks).[9] The weight average molecular weight (M_w) and polydispersity (M_w/M_n) were determined by high-temperature gel permeation chromatography in trichlorobenzene using a Waters 150-C GPC calibrated with polystyrene standards and converted to PP equivalents without further correction for ethylene content.

Thin films were prepared by spin casting 5 wt % polymer solutions in *n*-hexane onto IR grade fused silica substrates. After casting, the films were annealed at 70 °C for 12 h. Films were measured by AFM to have thickness between 200 and 300 nm.

Sum Frequency Generation Vibrational Spectroscopy. Surface vibrational spectra were obtained by sum frequency generation (SFG) vibrational spectroscopy. Briefly, surface vibrational spectra of the polymers were collected using the geometry shown in Figure 2. A visible and a tunable infrared laser beam were overlapped on the surface of a polymer film at incident angles of 50° and 55° with respect to the *z*-axis shown in Figure 2, and the induced sum-frequency signal was measured in the reflected direction. The visible beam (ω_{vis}) is 532 nm light generated by frequency doubling the 1064 nm fundamental output from a Continuum YAG-PY61 laser (generating ~20 ps pulses at 20 Hz and 35mJ/pulse) through a KTP crystal. The tunable infrared beam (ω_{IR}) is generated from a Laservision OPG/OPA (optical parametric generation)/(optical parametric amplification) system composed of two counter-rotating KTP crystals driven by a portion of the 532 nm light. The idler output of the OPG/OPA stage is mixed with some of the fundamental 1064 nm light in a difference frequency mixing stage comprised of two counter-rotating KTA crystals to generate a tunable IR source from 1900 to 4000 cm^{-1}. Surface vibrational spectra were obtained by tuning the infrared beam and measuring the sum-frequency signal as a function of the infrared frequency. The sum-frequency output signal ($\omega_{sum} = \omega_{vis} + \omega_{IR}$) was collected by a gated integrator and photon counting system.

Many additional details regarding vibrationally resonant SFG can be found in recent publications by Shen.[10−12] In general, the sum frequency signal is given by eq 1 and is proportional to the square of the second-order nonlinear susceptibility of the media, $\chi^{(2)}$. For vibrationally resonant SFG, $\chi^{(2)}$ is divided into the two terms described in eq 2. The first term, $\chi_{NR,}$ contains nonresonant contributions to the measured sum frequency intensity. The second term, the vibrationally resonant term, contains the vibrational mode strength ($\boldsymbol{A}_{q,}$), a damping term (Γ_q), and is maximized when the infrared beam (ω_{IR}) is tuned near a vibrational mode of one of the surface species (ω_q).

$$I(\omega_{sum}) \propto |\chi^{(2)}|^2 \tag{1}$$

$$I(\omega_{sum}) \propto \left|\chi_{NR} + \sum_q \frac{A_q}{\omega_{IR} - \omega_q + i\Gamma_q}\right|^2 \tag{2}$$

The vibrationally resonant mode strength, $\boldsymbol{A}_q$, is related to the hyperpolarizability of the vibrational resonance, β_q, in eq 3 by the number density of contributing oscillators, *n*, and an orientation averaged coordinate transformation where *I*,*J*,*K* refers to the laboratory fixed *x*,*y*,*z* coordinates and *i*,*j*,*k* refers to the internal *a*,*b*,*c* coordinates of the oscillator.

$$A_{q,IJK} = n\sum_{ijk}\langle(\hat{I}\cdot\hat{\imath})(\hat{J}\cdot\hat{\jmath})(\hat{K}\cdot\hat{k})\rangle\beta_{q,ijk} \tag{3}$$

The hyperpolarizability is interpreted in eq 4 as the product of the polarizability (α_{ij}) and dipole (μ_k) derivatives and gives the constraint that the vibrational mode (*Q*) must be both IR and Raman active for a sum frequency signal to be resonantly enhanced.

$$\beta_{q,ijk} \propto \frac{d\alpha_{ij}}{dQ}\cdot\frac{d\mu_k}{dQ} \tag{4}$$

This constraint leads to the well-known selection rule that species exhibiting inversion symmetry do not contribute to the sum frequency signal and that only those species lacking inversion symmetry give rise to an SFG signal. Additionally,

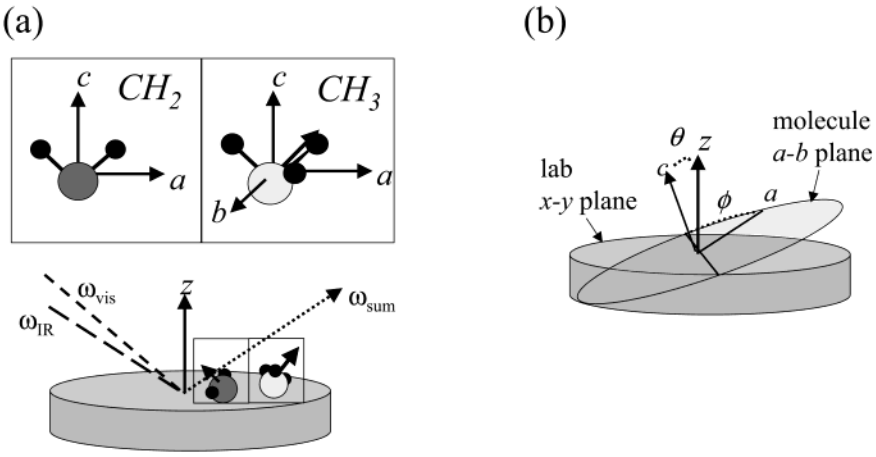

Figure 2. (a) Schematic showing beam geometry in SFG experimental setup and the molecular coordinate systems used in describing the CH_2 and the CH_3 groups. (b) Relationship between the molecular (*a*,*b*,*c*) and lab fixed (*x*,*y*,*z*) coordinate systems: For an $x-y$ isotropic surface the angle θ reflects a rotation about the molecule fixed *b*-axis and the angle ϕ is a final rotation about the molecule *c*-axis.

because the orientation average denoted by the brackets in eq 3 decays to zero as the distribution function describing the orientation of the molecules becomes wider, amorphous polymers, where the chain segments in the bulk are randomly oriented, have "effective" bulk inversion symmetry. The resonant sum frequency signal is expected to originate only from those chain segments that show preferential ordering at the interface.

Because only portions of a polymer chain are likely to be at the interface, the segments at the surface are treated as a collection of independent monomers rather than as an extended polymer. The surface is approximated as a collection of backbone CH_2 groups exhibiting some preferred orientation and side branch CH_3 groups exhibiting some other preferred direction. Thus in eq 3, $\beta_{q,ijk}$ refers to the hyperpolarizability components of a single CH_2 or CH_3 unit whose measured value is averaged over a distribution of orientations with respect to the beam-fixed lab coordinates. In the results presented here, Gaussian functions are used to describe the distribution of orientations.

The internal coordinate systems used to describe the methylene group and the methyl group are defined in Figure 2 as are the rotation angles θ and ϕ which relate the laboratory-fixed coordinate system to the molecular internal coordinate systems. In all calculations, the surface of the polymer films is assumed to be isotropic in the surface plane and the azimuthal angle (not shown) has been integrated over its full range of values.

Spectra were collected in the C−H stretching region using the $s_{sum}s_{vis}p_{ir}$ polarization combination, which specifically probes the *yyz* component of $\boldsymbol{A}_q$.[10] This polarization combination is most sensitive to vibrations that have a component of the vibrational dipole (μ_k) along the surface normal, *z*, and a component of the polarizability tensor (α_{ij}) in the surface plane $(x-y)$. Additional spectra were collected using the $s_{sum}p_{vis}s_{ir}$ polarization combination, which is sensitive to the *yzy* component of $\boldsymbol{A}_q$. After normalization, experimental data is fit to eq 2 in order to extract values for $\boldsymbol{A}_q$. If the components of β_{ijk} for each vibrational resonance are known, then the fitted mode strengths can be used in eq 3 to determine changes in number density and orientation of CH_2 and CH_3 groups at the top layer of the surface contributing to the sum frequency signal.

Results

SFG Spectra of Poly(ethylene-*co*-propylene) Rubber (*a*EPR) Series. SFG spectra for atactic polypropylene (*a*PP1) and three of the poly(ethylene-*co*-propylene) rubber copolymers (*a*EPR4, *a*EPR5, and *a*EPR7) using the *ssp* polarization combination are shown in Figure 3. The feature at 2883 cm^{-1} in the *a*PP1 spectra is the strongest feature in the series. The SFG spectra of each of the other *a*EPR copolymers have been normalized, using the peak at 2883 cm^{-1} from *a*PP1 as a reference value. Thus in the analysis that follows, all chemical concentrations derived from the SFG spectra are relative to the surface composition of *a*PP1.

The spectra of *a*PP1 is similar to previously published spectra.[3] The features at 2850 cm^{-1} and 2920 cm^{-1} are assigned as the CH_2 symmetric (CH_2(s)) and antisymmetric (CH_2(a)) stretches, respectively, from the polymer backbone. Features at 2883 cm^{-1} and the shoulder at 2968 cm^{-1} are assigned to the CH_3 symmetric (CH_3(s)) and antisymmetric (CH_3(a)) stretches from the methyl side branch. An additional feature at 2940 cm^{-1} arises from the Fermi resonance between the CH_3(s) and an overtone of the CH_3 antisymmetric bending mode.

The *ssp* spectra of the *a*EPR copolymers in the series contain the same features as *a*PP1, however the CH_2(s) stretch becomes more intense relative to the CH_3(s) stretch as the ethylene weight fraction increases. SFG spectra of *a*EPR2 and *a*EPR3 (not shown) are intermediate to *a*PP1 and *a*EPR4 and the SFG spectra of *a*EPR6 is intermediate to *a*EPR5 and *a*EPR7.

Figure 4 shows the SFG spectra for the copolymers using the *sps* polarization combination. The CH_3(a) peak is the dominant feature for each copolymer. As the ethylene fraction increases, a broad region from 2890 to 2940 cm^{-1} which contains contributions from the CH_3(s), CH_2(a), and methyl Fermi resonance increases in intensity. Solid lines in Figures 3 and 4 represent best fits to the data using eq 2 and fitting to five peaks where A_q is the normalized mode strength, ω_q is the position of the vibrational peak, and Γ_q is the damping factor for the vibration (between 11 and 13 cm^{-1} for all peaks). The fitted and normalized mode strengths are given in Table 2 for both polarization combinations (*ssp* and *sps*). Error bars in the fitted mode strengths are derived from the components of the second derivative inverse curvature matrix used in the spectra fitting routine.

Comparing the two extremes in the series, *a*PP1 and *a*EPR7, there is an ~40% decrease in the bulk methyl number density. However, the SFG vibrational mode strengths for the *ssp* CH_3(s) and CH_3(a) peaks decrease by less than 20%. Additionally, the CH_2 bulk concentration increases by ~40% between *a*PP1 and *a*EPR7, but the CH_2(s) *ssp* mode strength increases by nearly 100%. From eq 3, it can be seen that in the absence of orientation changes, the SFG mode strengths are expected

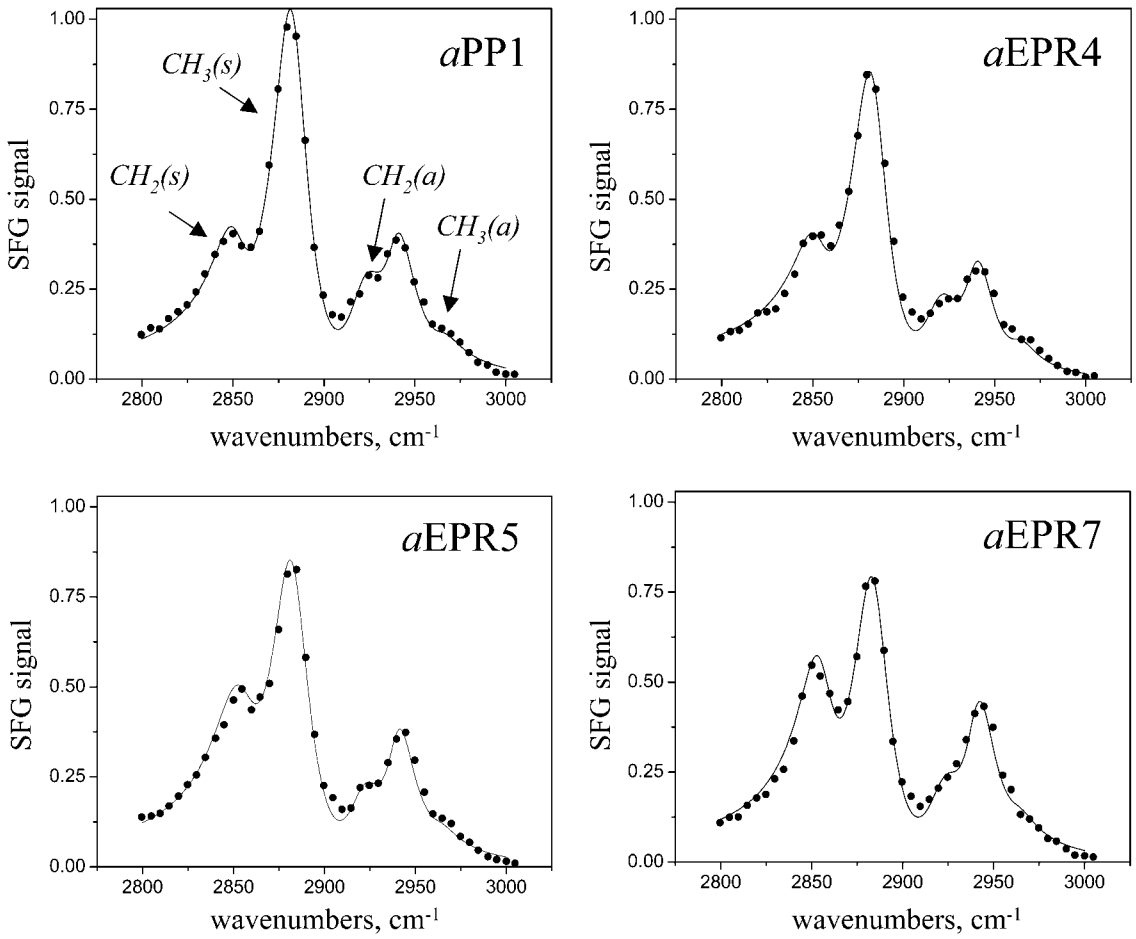

Figure 3. SFG spectra of *a*PP1 and *a*EPR copolymers (*ssp* polarization combination). All of the spectra have been normalized using the peak at 2883 cm^{-1} for *a*PP1 (the strongest peak in the series) as a reference. Solid lines represent best fits to eq 2.

to vary linearly with number density. That the CH_2(s) and CH_3(s) vibrational mode strengths do not vary linearly with number density is an immediate indication that there are significant changes in polymer composition and orientation at the interface as the bulk copolymer composition is varied.

The ratio of A_q for the CH_2(s) stretch (~2850 cm^{-1}) to A_q for the CH_3(s) stretch (~2883 cm^{-1}) as a function of the bulk CH_2 to CH_3 mole ratio for the *a*PP and the *a*EPR series is plotted in Figure 5. This mode strength ratio increases with composition in a roughly linear fashion over the copolymer compositional range we have investigated and would seem to indicate that the surface composition changes linearly with the bulk composition. However, because the individual mode strengths depend on both the number density and the orientation of the contributing molecules, the ratio of the CH_2 and CH_3 SFG mode strengths given in eq 5 reflects a convolution of the ratios of the concentration and orientation.

$$\frac{A_{CH_2(s)}(ssp)}{A_{CH_3(s)}(ssp)} = \left(\frac{n_{CH_2}\langle\beta_{CH_2,yyz}\rangle}{n_{CH_3}\langle\beta_{CH_3,yyz}\rangle}\right)_{surface} \quad (5)$$

To deconvolute the relative contributions from the number density of molecules, n, and from the orientation average, $\langle\beta_{q,yyz}\rangle$, it is necessary to know how the methylene group orientation and the methyl group orientation change as a function of copolymer composition. The following two sections discuss these orientation changes.

Methylene Orientation. Strategies for determining molecular orientation from SFG data have been discussed in detail elsewhere.[10] For a vibrational resonance to be visible in spectra with *ssp* polarization requires that a component of the vibrational dipole lie in the *z* direction, normal to the surface plane (see Figure 2). The vibrational dipole for the CH_2(s) stretch lies along the molecule symmetry *c*-axis, and the dipole for the CH_2(a) stretch lies perpendicular to it along the molecule fixed *a*-axis. Figure 6 shows a plot of the *ssp* mode strength ratio of the CH_2(s) stretch to the CH_2(a) stretch as a function of copolymer composition. The mode strengths in Table 2 show that the magnitude of the symmetric stretch increases relative to the asymmetric stretch as ethylene concentration increases—an indication that the CH_2 *c*-axis becomes more oriented toward the surface normal.

Additionally, for a vibrational resonance to be visible in *sps* polarization combination requires that a component of the dipole moment lie in the surface plane. That the CH_2(s) mode strength is very small in all of the *sps* spectra and that the CH_2(a) mode strength increases in magnitude at high ethylene concentration supports the suggestion that the CH_2 symmetry *c*-axis orients toward the surface normal as ethylene concentration increases.

Quantitatively, the average orientation and orientation distribution of the CH_2 groups contributing to the sum frequency signal can be calculated using the ratio of the symmetric and antisymmetric mode strengths from the *ssp* spectra, eq 6, and by knowing the relationships between the hyperpolarizability tensor components for each vibrational stretch. By taking the

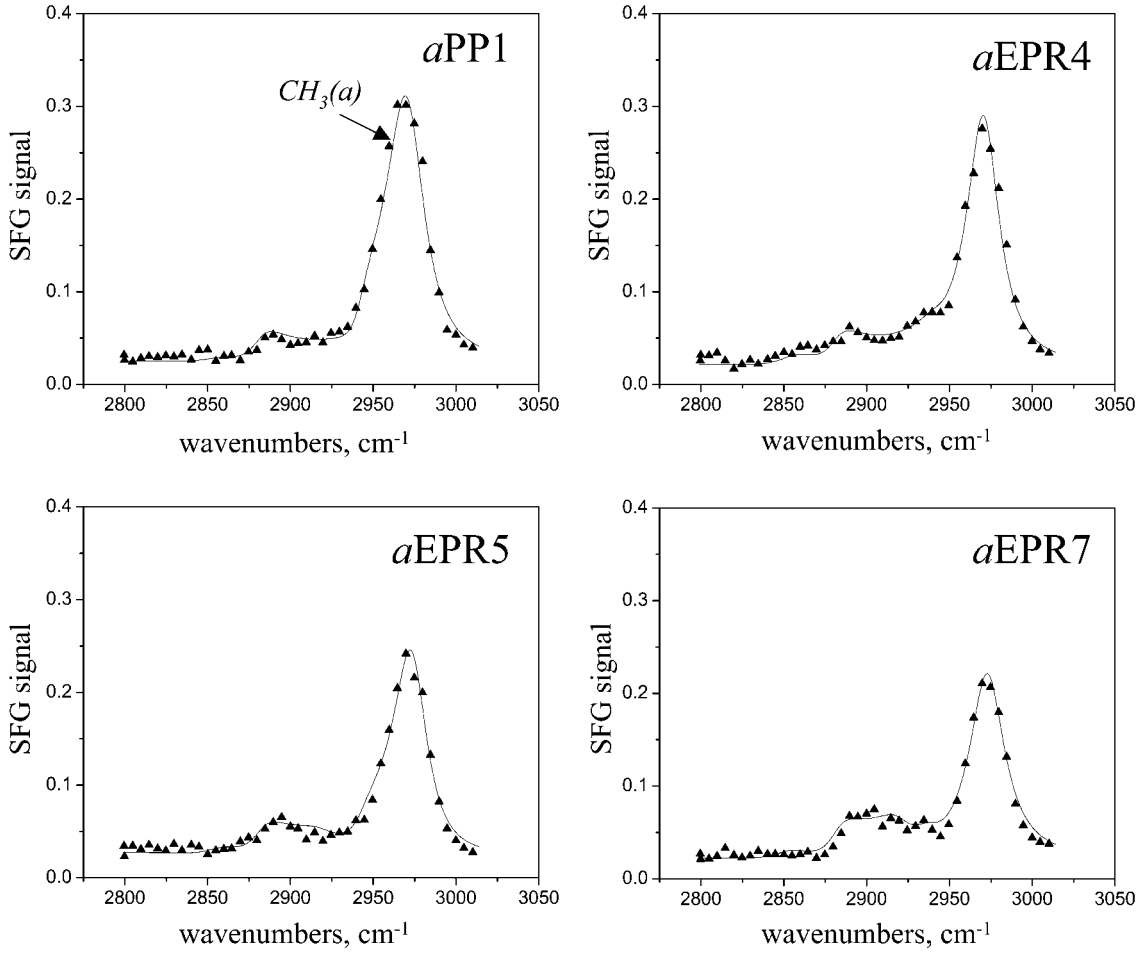

Figure 4. SFG spectra of *a*EPR copolymers (*sps* polarization combination). Solid lines represent best fits to eq 2.

TABLE 2: Individual Vibrational Mode Strengths Derived from SFG Spectra Using Equation 2[a]

	mole fraction ethylene	CH_2(s) ~ 2850 cm^{-1}		CH_3(s) ~ 2883 cm^{-1}		CH_2(a) ~ 2920 cm^{-1}		Fermi ~ 2940 cm^{-1}		CH_3(a) ~ 2968 cm^{-1}	
		ssp	*sps*	*ssp*	*sps*	*ssp*	*sps*	*ssp*	*sps*	*ssp*	*sps*
*a*PP1	0	3.09 ± 0.13	1.0 ± 0.5	10.94 ± 0.06	2.1 ± 0.6	3.8 ± 0.2	1.3 ± 0.6	3.8 ± 0.2	1.7 ± 0.8	0.7 ± 0.2	−7.1 ± 0.2
*a*EPR2	0.069	3.22 ± 0.15		10.75 ± 0.06		3.7 ± 0.2				0.7 ± 0.2	
*a*EPR3	0.103	3.17 ± 0.15		10.75 ± 0.06		3.6 ± 0.2				0.7 ± 0.2	
*a*EPR4	0.190	3.30 ± 0.16	0.2 ± 0.2	10.35 ± 0.09	2.2 ± 0.6	3.4 ± 0.2	1.5 ± 0.7	3.8 ± 0.2	1.1 ± 0.5	0.9 ± 0.2	−6.6 ± 0.2
*a*EPR5	0.277	4.3 ± 0.2	1.4 ± 0.7	10.03 ± 0.08	2.1 ± 0.5	3.6 ± 0.2	−3.0 ± 1.8	4.3 ± 0.2	3.4 ± 0.8	0.6 ± 0.2	−6.2 ± 0.2
*a*EPR6	0.344	4.9 ± 0.2		9.87 ± 0.08		3.5 ± 0.2				0.6 ± 0.2	
*a*EPR7	0.417	5.5 ± 0.2	1.1 ± 0.5	9.55 ± 0.08	2.0 ± 0.6	3.6 ± 0.2	−3.5 ± 1.6	4.6 ± 0.2	3.2 ± 1.2	0.6 ± 0.2	−5.9 ± 0.2

[a] Reported magnitudes of the mode strengths are relative values—where the SFG spectra have been normalized such that the CH_3(s) stretch from *a*PP1 (2883 cm^{-1}) has an SFG intensity of 1.

ratio of two modes from the same species, the number densities cancel, leaving a ratio that is dependent only on the orientation of the species.

$$\frac{A_{CH_2(s)}(ssp)}{A_{CH_2(a)}(ssp)} = \frac{\langle\beta_{CH_2(s),yyz}\rangle}{\langle\beta_{CH_2(a),yyz}\rangle} \tag{6}$$

For the CH_2(s) stretch there are 3 components (β_{aac}, β_{bbc}, *and* β_{ccc}) and for the CH_2(a) symmetric stretch there are 2 terms ($\beta_{aca} = \beta_{caa}$) which have been shown to satisfy the following relationships:[10]

$$\beta_{aac} \approx 5.13\beta_{bbc} \approx 1.64\beta_{ccc} \approx 1.24\beta_{aca}$$

Because the thin films were spin cast and then annealed for several hours above T_g, it is assumed that the surface is isotropic in the surface ($x-y$) plane. Using the method outlined by Hirose[13] and after inserting these values for β, eq 6, to a good approximation, can be shown to reduce for the *ssp* polarization combination to

$$\frac{A_{CH_2(s)}(ssp)}{A_{CH_2(a)}(ssp)} = \frac{12 \cdot \langle\cos\theta\rangle + \langle\cos 2\phi\rangle(\langle\cos\theta\rangle - \langle\cos 3\theta\rangle)}{2(\langle\cos\theta\rangle - \langle\cos 3\theta\rangle)(1 + \langle\cos 2\phi\rangle)} \tag{7}$$

where the tilt angle, θ, and twist angle, ϕ, are defined in Figure 2. For the spectra with *sps* polarization combination, the mode strength ratio between the CH_2(s) and CH_2(a) mode strengths can be reduced to

$$\frac{A_{CH_2(s)}(sps)}{A_{CH_2(a)}(sps)} = \frac{2(\langle\cos\theta\rangle - \langle\cos 3\theta\rangle)(1 + \langle\cos 2\phi\rangle) - 8 \cdot \langle\cos\theta\rangle}{\langle\cos 2\phi\rangle(\langle\cos\theta\rangle - \langle\cos 3\theta\rangle)} \tag{8}$$

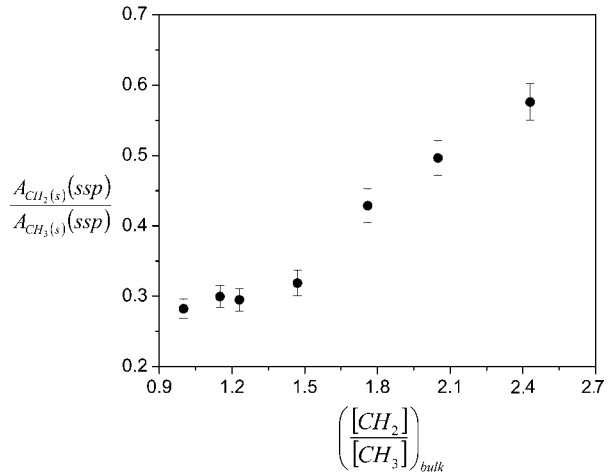

Figure 5. Ratio of CH_2(s)/CH_3(s) *ssp* vibrational mode strengths (A_q) as a function of the bulk [CH_2]/[CH_3] ratio for *a*PP1 and the *a*EPR series.

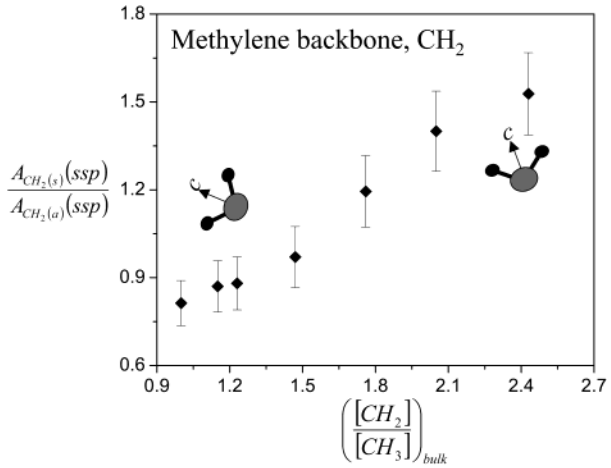

Figure 6. Ratio of CH_2(s)/CH_2(a) *ssp* vibrational mode strengths as a function of the bulk [CH_2]/[CH_3] ratio for *a*PP1 and the *a*EPR series. The inset CH_2 units denote that the CH_2 *c*-axis orients more toward the surface normal as the magnitude of this vibrational mode strength ratio increases.

Two similar types of relationships can be formed comparing the CH_2(s) *ssp* and *sps* mode strengths and comparing the CH_2(a) *ssp* to *sps* mode strengths (requiring use of Fresnel factors[10] to compare local field intensities of *s* and *p* 532 nm light and *p* and *s* mid-IR light at the air/polymer interface). Together, these 4 relationships allow us to place significant restrictions on the average orientation and orientation distribution of CH_2 groups.

Using Gaussian distributions for the angles θ and ϕ, best fits are obtained for all spectra using a narrow distribution for ϕ centered around 0° ($\phi_o = 0° \pm 10°$, $\Delta\phi = 10° \pm 10°$). This small value of ϕ indicates that the average CH_2 plane is perpendicular to the surface plane and that the average chain backbone is parallel to the surface plane. Under this constraint, the remaining parameters, θ_o and $\Delta\theta$, are found to vary from $62° \pm 8°$ with distribution width of $15° \pm 7°$ for *a*PP1 (the copolymer with no ethylene), to $30° \pm 11°$ with a distribution width of $20° \pm 15°$ for *a*EPR7 (the copolymer with the highest ethylene content).

Best-fit orientation parameters for all of the copolymers are given in Table 3. As the ethylene content increases, the average CH_2 symmetry axis *(c)* becomes more oriented toward the surface normal *(z)*. From these calculated orientation parameters,

TABLE 3: Best Fit Average Orientation Parameters of the CH_2 Unit for the *a*EPR Series[a]

	mole fraction ethylene	θ_o, °	$\Delta\theta$, °	ϕ_o, °	$\Delta\phi$, °	$\langle\beta_{CH_2(s),yyz}\rangle$
*a*PP1	0	62 ± 8	15 ± 7	0 ± 10	10 ± 10	0.16 ± 0.03
*a*EPR2	0.069	59 ± 8	15 ± 7	0 ± 10	10 ± 10	0.17 ± 0.03
*a*EPR3	0.103	58 ± 8	15 ± 8	0 ± 10	10 ± 10	0.18 ± 0.04
*a*EPR4	0.190	56 ± 9	20 ± 8	0 ± 10	10 ± 10	0.20 ± 0.05
*a*EPR5	0.277	52 ± 15	20 ± 15	0 ± 15	10 ± 20	0.22 ± 0.08
*a*EPR6	0.344	40 ± 20	25 ± 15	0 ± 15	10 ± 20	0.26 ± 0.08
*a*EPR7	0.417	30 ± 11	20 ± 15	0 ± 10	10 ± 10	0.32 ± 0.05

[a] The angles θ and ϕ are defined in Figure 2. The value of $\langle\beta_{CH_2(s),yyz}\rangle$ increases as the CH_2 *c*-axis orients more along the surface normal (*z*-axis).

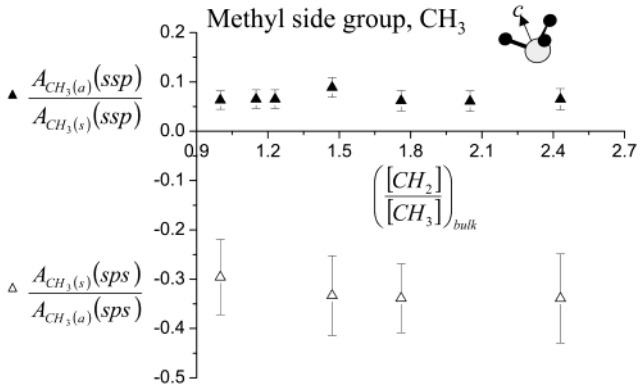

Figure 7. CH_3(a)/CH_3(s) *ssp* vibrational mode strength ratio (▲), and CH_3(s)/CH_3(a) *sps* vibrational mode strength ratio (△) as a function of the bulk [CH_2]/[CH_3] ratio for *a*PP1 and the *a*EPR series.

it is possible to ascertain how the relative value of $\langle\beta_{CH_2(s),yyz}\rangle$ varies from *a*PP1 to *a*EPR7. This value is also given in Table 3. A larger magnitude of $\langle\beta_{CH_2(s),yyz}\rangle$ indicates the CH_2 units are oriented with their *c*-axis more along the surface normal.

Methyl Orientation. The analysis of the average orientation and orientation distribution of the side-branch methyl group is similar to the analysis of the methylene unit. The vibrational dipole for the CH_3(s) stretch lies along the molecule symmetry *c*-axis, and the dipole for the CH_3(a) stretch lies perpendicular to it along the molecule fixed *a*-axis. Since the CH_3(s) stretch is much larger than the CH_3(a) stretch for each copolymer in the *ssp* spectra we can infer that the average methyl symmetry axis lies more or less along the surface normal. An upright methyl orientation configuration is consistent with the observation that the C−H stretch is absent from the spectra. Assuming tetrahedral bonding for the backbone carbons, if the average methyl group is oriented upright, then the average C−H group should lie more or less in the surface plane. For an azimuthally symmetric surface, neither the *ssp* nor the *sps* polarization combinations will be very sensitive to measuring vibrations that are in the surface plane.

The *sps* spectra also support the interpretation of an upright methyl group since the CH_3(a) stretch is much larger in this polarization combination than the CH_3(s) stretch. Changes in the methyl group orientation can be qualitatively assessed by plotting out the ratios of the CH_3(s) to CH_3(a) mode strengths as a function of copolymer composition for both polarization combinations (Figure 7). These two ratios remain relatively unchanged as a function of ethylene concentration, which indicates that the methyl orientation remains fixed as the copolymer composition is varied. This implies that the value of $\langle\beta_{CH_3(s),yyz}\rangle$ can be approximated as a constant for *a*PP1 and all of the *a*EPR samples.

TABLE 4: Concentrations of CH_3 and CH_2 Groups Contributing to the Sum Frequency Signal for the aEPR Copolymers, Relative to aPP1 (3rd and 5th columns) and Surface Excess/Depletion Values Obtained after Normalizing to the Bulk Compositions (4th and 6th columns)

sample	mole fraction ethylene	relative CH_3 surface concn $n_{CH_3,aEPRx}/n_{CH_3,aPP1}$	CH_3 surface excess $n_{CH_3,surface}/[CH_3]_{bulk}$	relative CH_2 surface concn $n_{CH_2,aEPRx}/n_{CH_2,aPP1}$	CH_2 surface depletion $n_{CH_2,surface}/[CH_2]_{bulk}$
*a*PP1	0	1	1	1	1
*a*EPR2	0.069	0.983 ± 0.011	1.056 ± 0.012	1.0 ± 0.2	0.9 ± 0.2
*a*EPR3	0.103	0.983 ± 0.011	1.092 ± 0.012	0.9 ± 0.2	0.8 ± 0.2
*a*EPR4	0.190	0.946 ± 0.013	1.168 ± 0.017	0.9 ± 0.3	0.7 ± 0.2
*a*EPR5	0.277	0.917 ± 0.012	1.273 ± 0.017	0.9 ± 0.3	0.7 ± 0.3
*a*EPR6	0.344	0.902 ± 0.012	1.367 ± 0.019	0.9 ± 0.3	0.7 ± 0.2
*a*EPR7	0.417	0.873 ± 0.012	1.48 ± 0.02	0.89 ± 0.17	0.63 ± 0.12

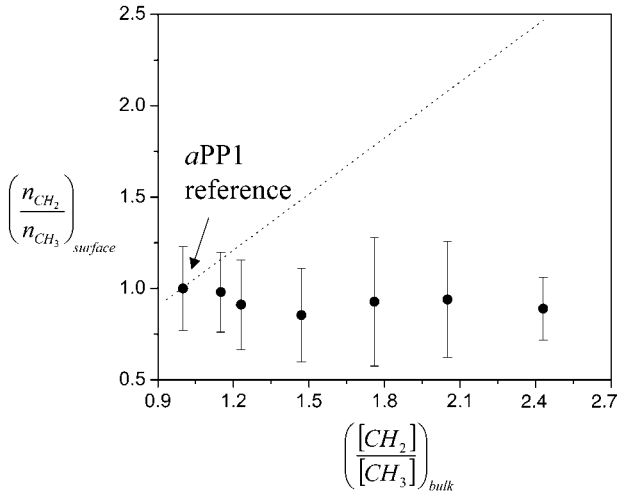

Figure 8. Plot of surface (n_{CH_2}/n_{CH_3}) contributing to the SFG signal vs the bulk $[CH_2]/[CH_3]$ concentration ratio generated after removing the orientation effects from the CH_2(s) and CH_3(s) *ssp* vibrational mode strengths: data points are normalized to *a*PP1 which is given a surface (n_{CH_2}/n_{CH_3}) ratio and a bulk $[CH_2]/[CH_3]$ ratio of 1. The dashed line shows the dependence that would be expected in the absence of surface segregation effects.

To quantify the methyl orientation, the mode strengths have been fit in a procedure analogous to the fitting of the methylene mode strengths. From the analysis, a best-fit tilt angle, θ_c, of 20−30 degrees with a distribution width of 20 degrees is calculated for the methyl group orientation.

Surface Composition of *a*EPR Series. Knowing how the methyl and methylene orientations change with bulk composition and consequently how $\langle\beta_{CH_2(s),yyz}\rangle$ and $\langle\beta_{CH_3(s),yyz}\rangle$ change, the relationship between the CH_2(s) and CH_3(s) mode strengths can be reanalyzed. Inserting the relative values of $\langle\beta_{q,yyz}\rangle$ for each copolymer into eq 5 removes orientation effects from the mode strength ratio and a new relationship can be made which directly relates the ratio of (n_{CH_2}/n_{CH_3}) contributing to the sum frequency signal at the surface to the bulk $[CH_2]/[CH_3]$ ratio.

Figure 8 is a plot of the surface (n_{CH_2}/n_{CH_3}) ratio vs the bulk $[CH_2]/[CH_3]$ ratio for the *a*EPR series accounting for the orientation effects. Because of the initial spectral normalization scheme, all of the surface (n_{CH_2}/n_{CH_3}) ratios are in reference to the surface (n_{CH_2}/n_{CH_3}) ratio for *a*PP1. The graph shows that as the bulk ethylene mole fraction increases, the ratio of CH_2 to CH_3 units contributing to the sum frequency signal does not change within the error of the measurement. The dotted line in Figure 8 shows the trend that would be observed if the surface composition changed linearly with the bulk composition. This indicates that as the bulk ethylene content increases, there is either an excess of CH_3 units or a depletion of CH_2 units contributing to the sum frequency signal, relative to the bulk compositions.

Relative changes in concentration of methyl groups contributing to the sum frequency signal as a function of bulk composition can be estimated from a direct comparison of the methyl mode strengths from Table 2. Since the data presented in Figure 7 implies that the methyl orientation does not significantly change as the bulk composition varies, the change in magnitude of the CH_3 mode strengths between *a*PP1 and *a*EPR7 must come primarily from changes in CH_3 number density.

Table 4 summarizes the *a*EPR copolymer surface methyl compositions relative to aPP1. The relative CH_3 concentrations are generated from the simple ratio of the $A_{CH_2(s),ssp}$ between the *a*EPR samples and the *a*PP1 reference sample. Relative surface excess values are calculated by normalizing the relative surface concentrations to the corresponding bulk composition ratio (eq 9).

$$\left(\frac{n_{CH_3,surface}}{[CH_3]_{bulk}}\right)_{relative\ to\ aPP1} = \frac{(A_{CH_3(s)}(ssp)/[CH_3]_{bulk})_{aEPRx}}{(A_{CH_3(s)}(ssp)/[CH_3]_{bulk})_{aPP1}} \quad (9)$$

Relative to *a*PP1, *a*EPR7 orients ∼13% fewer methyl side branches at the surface. After taking into account differences in bulk composition, however, *a*EPR7 actually orients ∼50% more methyl side branches than *a*PP1. A methyl surface excess can only partially account for the overall depletion of the surface CH_2/CH_3 ratio. In addition to a relative excess of methyl groups contributing to the sum frequency signal, there must also be a relative decrease in the number of backbone CH_2 units contributing to the signal. Relative CH_2 concentrations and depletions for the *a*EPR copolymers are calculated in the same way as the methyl surface excesses are also presented in Table 4. The table shows that in addition to the methyl group surface excess, *a*EPR7 has a relative depletion about 30% of CH_2 groups contributing to the sum frequency signal.

While this may be directly interpreted as meaning that there are fewer CH_2 units present at the surface, a decrease in CH_2 units contributing to the SFG signal can also be accounted for by dipole cancellation of adjacent CH_2 units in a trans configuration. For example, SFG spectra of alkyl chain self-assembled monolayers typically have very small intensities from the CH_2 backbone units relative to the overall concentration of CH_2 units—even though the CH_2 groups are well ordered. The small magnitude of the peaks is generally attributed to cancellation of the SFG signal from pairs of methylene units in a trans configuration, which exhibit local inversion symmetry.[14] Most of the CH_2 signal in these systems arises from gauche defects in the chains.

If the ethylene units inserted into the *a*EPR backbone are primarily in trans configurations, then they exhibit a similar type of local inversion symmetry as the monolayer alkyl chain and may at least partially cancel with one another. Because the CH_2 units were shown to become more ordered with the *c*-axis

toward the surface normal and with the CH_2 plane perpendicular to the surface plane as the ethylene content increased, indicates that the chain backbones tend to lie somewhat in the surface plane and that many of the chain segments at the surface are likely in a trans configuration. Thus it is more likely that there is a depletion of CH_2 groups contributing to the signal through some sort of cancellation process than it is that there is an actual depletion of CH_2 groups at the surface.

In the extreme case, where every ethylene unit at the surface is in a trans configuration, and complete trans cancellation occurs, all of the SFG signal from the ethylene units would cancel and only SFG signal arising from the propylene units at the surface would be measured. If this were the case and the surface was comprised of a statistical mixture of CH_2 and CH_3 groups, n_{CH_2}/n_{CH_3} contributing to the SFG signal would be invariant with respect to copolymer composition − assuming no segregation of methyl groups. Taking into account the surface excess of n_{CH_3} as the bulk ethylene concentration increases, would lead to an overall negative dependence of $(n_{CH_2}/n_{CH_3})_{surface}$ on the bulk composition. That a negative dependence is not observed in Figure 8 indicates that at most there can be only a partial cancellation of ordered CH_2 groups at the surface leading to a slightly reduced CH_2 intensity for the ethylene-containing copolymers.

Discussion

The preceding analysis of the SFG spectra places significant restrictions on the average orientation of CH_2 and CH_3 units at the surface and thus on the possible conformations of the *a*EPR chain segments at the air−polymer interface. A schematic diagram incorporating the experimentally determined tilt angles for the CH_2 and CH_3 units, showing the primary differences in surface chain segment configurations for *a*PP1 and *a*EPR7, is presented in Figure 9.

Although *a*PP1 has more methyl groups (denoted by the white circles) ordered at the interface than *a*EPR7, steric hindrances between adjacent methyl groups prevent *a*PP1 from orienting every methyl group away from the surface. In the *a*PP polymer segment shown, 4 out of the 6 methyl groups have been oriented out of the surface at average tilt of 30 degrees. The 2 remaining methyl groups are randomly oriented or oriented toward the bulk. By preferentially ordering the methyl groups, the orientation of the methylene backbone units is restricted. The backbone units are forced to orient with larger, possibly more random, tilt angles.

As the methyl concentration is diluted by the incorporation of ethylene in the backbone, steric hindrances between adjacent methyl groups are reduced and the polymer can place a higher percentage of methyl groups at the surface. In the *a*EPR7 polymer segment shown, all of the methyl groups are oriented away from the surface. Additionally, because the concentration of methyl units is diluted, the methylene units adopt more trans configurations and orient CH_2 groups more toward the surface normal.

These surface configurations are supported by simulations of the atactic polypropylene (*a*PP) surface performed by Mansfield and Theodorou,[15] and of the polyethylene (PE) surface performed by Mattice.[16] Both simulations predict that chain backbones near the surface (top 5−10 Å) tend to lie in the surface plane in order to maximize the cohesive energy between the polymer units at the surface and in the bulk. Specifically for *a*PP, the simulations also predicted that the methyl side group would adopt an orientation that would orient it away from the surface. Comparing between the two polymers,

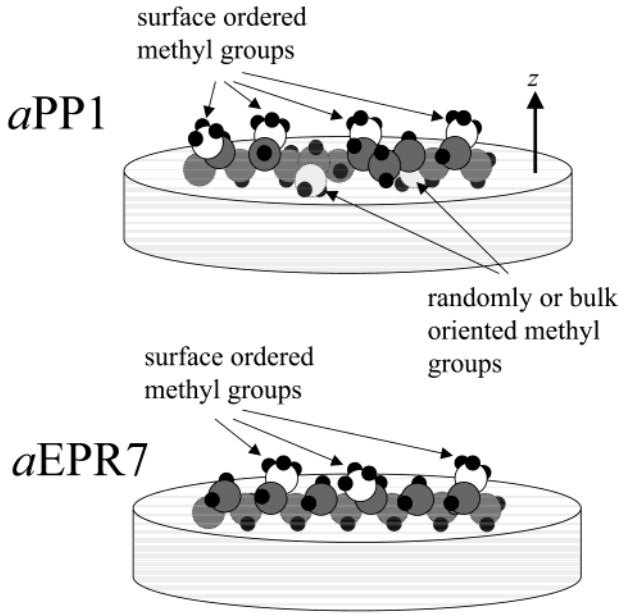

Figure 9. Schematic of proposed structures of *a*PP1 and *a*EPR7 surfaces. For clarity of presentation backbone carbon atoms are denoted by gray shaded circles and side branch methyl carbon atoms are denoted by open/white circles. ***a*PP1:** The *a*PP1 surface has a percentage of methyl groups that are preferentially oriented away from the bulk (66% in the example shown). The remaining methyl groups do not contribute significantly to the SFG signal and are either randomly oriented or oriented toward the bulk. ***a*EPR7:** Reduced steric hindrances allow *a*EPR7 to orient a relatively higher percentage of methyl groups away from the bulk (100% in the example shown). Additionally, more of the backbone atoms are in a trans conformation.

the calculated order parameter for the backbone C−C bond direction is smaller for *a*PP than PE. This may indicate that PE has longer runs of chain segments in the surface plane and that it may have a higher number density of chain segments in a trans configuration at the surface than *a*PP.

The phenomenon of orienting methyl groups away from the surface has several possible explanations. The first is that air is a hydrophobic media, and thus the more hydrophobic methyl groups should be attracted to the interface. The second is the density change at the interface. The lower density on the air-side of the interface allows the polymers to extend bulky side groups away from the surface. This is a general type of effect that has also been observed on polyimide,[5] polystyrene,[6] and poly(methyl)methacrylate[18] by SFG. At interfaces where both media have similar densities (polymer/solid) or specific interactions (polymer/liquid), the effect may be expected to be suppressed. Theoretical calculations of *a*PP at the air/graphite interface suggest that the ordering of methyl groups at this interface is much lower than the air/polymer interface.[17] Recent experimental evidence on the polymethacrylate polymers[18] and polystyrene[4] suggests that preferential ordering of side groups can be suppressed at the polymer/liquid interface.

The tendency to order side branches out of the surface may also give some additional insight into the higher surface activity of branched polyolefins. In blends of branched polyolefins, there is typically an enrichment of the component with the higher degree of branching at the air/polymer interface.[1,19] Explanations have been given on the basis of the lower cohesive energy (and lower surface tension) of the higher branched component.[1] The results of this study suggest that in addition to the cohesive energy, there are specific interactions at the air/polymer interface that tends to order the side branches out of the surface. Thus, in blends of polymers with different degrees of side branching,

the polymer with the higher number densities of branches would be expected at the air/polymer interface. Any segregation based on this effect would work in parallel with cohesive energy contributions and other entropic factors.

Conclusion

Sum frequency generation vibrational spectroscopy has been used to quantify the effect of branching on the surface chain conformation of a series of aspecific ethylene−propylene copolymers. The results show that methyl side branches prefer to orient away from the surface regardless of copolymer composition. The incorporation of ethylene units decreases the steric hindrance between adjacent methyl groups. The reduced steric effects are proposed to allow ethylene-rich copolymers to assume configurations that orient a surface excess of methyl groups away from the surface. Increasing the number of ethylene units in the backbone also allows the CH_2 units in the backbone to orient with their symmetry axis along the surface normal.

Acknowledgment. This work was supported by the Director, Office of Science, Office of Basic Energy Sciences, Division of Materials Science and Engineering, of the U.S. Department of Energy under Contract No. DE-AC03-76SF00098 and by Basell Polyolefins. The authors acknowledge polymer synthetic assistance from Robert L. Jones, and material characterization assistance from Debby Morgan, Alexander Marchione, Dr. Bill Long, and Dr. Robert Zeigler.

References and Notes

(1) Scheffold, F.; Budkowski, A.; Steiner, U.; Eiser, E.; Klein, J.; Fetters, L. J. *J. Chem. Phys.* **1996**, *104*, 8795.
(2) Wei, X.; Hong, S. C.; Lvovsky, A. I.; Held, H.; Shen, Y. R. *J. Phys. Chem B* **2000,** *104*, 3349.
(3) Zhang, D.; Shen, Y. R.; Somorjai, G. A. *Chem. Phys. Lett.* **1997**, *281*, 394.
(4) Gautam, K. S.; Schwab, A. D.; Dhinojwala, A.; Zhang, D.; Dougal, S. M.; Yeganeh, M. S. *Phys. Rev. Lett.* **2000**, *85*, 3854.
(5) Briggman, K. A.; Stephenson, J. C.; Wallace, W. E.; Richter, L. J. *J. Phys. Chem. B* **2001**, *105*, 2785.
(6) Oh-e, M.; Lvovsky, A. I.; Wei, X.; Shen, Y. R. *J. Chem. Phys.* **2000**, *113*, 8827.
(7) Gracias, D. H.; Zhang, D.; Lianos, L.; Ibach, W.; Shen, Y. R.; Somorjai, G. A. *Chem. Phys.* **1999**, *245*, 277.
(8) Resconi, L.; Jones, R. L.; Rheingold, A. L.; Yap, G. P. *Organometallics* **1996**, *15*, 998.
(9) Koenig, J. L. *Chemical Microstructure of Polymer Chains*; John Wiley & Sons: New York, 1982.
(10) Wei, X.; Hong, S. C.; Zhuang, X. W.; Goto, T.; Shen, Y. R. *Phys. Rev. E* **2000**, *62*, 5160.
(11) Miranda, P. B.; Shen, Y. R. *J. Phys. Chem. B* **1999**, *103*, 3292.
(12) Zhuang, X.; Miranda, P. B.; Kim, D.; Shen, Y. R. *Phys. Rev. B* **1999**, *59*, 12632.
(13) Hirose, C.; Akamatsu, N.; Domen, K. *Appl. Spectrosc.* **1992**, *46*, 1051.
(14) Casson, B. D.; Bain, C. D. *J. Phys. Chem. B* **1999**, *103*, 4678.
(15) Mansfield, K. F.; Theodorou D. N. *Macromolecules* **1990**, *23*, 4430.
(16) He, D. Y.; Reneker, D. H.; Mattice, W. L. *Polymer* **1997**, *38*, A19.
(17) Mansfield, K. F.; Theodorou, D. N. *Macromolecules* **1991**, *24*, 4295.
(18) Wang, J.; Woodcock, S. E.; Buck, S. M.; Chen, C.; Chen, Z. *J. Am. Chem. Soc.* **2001**, *123*, 9470.
(19) Opdahl, A.; Phillips, R. A.; Somorjai, G. A. *Macromolecules*, in press.